CrossMark

Impedance feedback control of microfluidic valves for reliable post processing combinatorial droplet injection

Brant Axt[1] · Yi-Fan Hsieh[2] · Divya Nalayanda[1] · Tza-Huei Wang[1,2]

Abstract Droplet microfluidics has found use in many biological assay applications as a means of high-throughput sample processing. One of the challenges of the technology, however, is the ability to control and merge droplets on-demand as they flow through the microdevices. It is in the interest of developing lab-on-chip devices to be able to combinatorically program additive mixing steps for more complex multistep and multiplex assays. Existing technologies to merge droplets are either passive in nature or require highly predictable droplet movement for feedforward control, making them vulnerable to errors during high throughput operation. In this paper, we describe and demonstrate a microfluidic valve-based device for the purpose of combinatorial droplet injection at any stage in a multistep assay. Microfluidic valves are used to robustly control fluid flow, droplet generation, and droplet mixing in the device on-demand, while on-chip impedance measurements taken in real time are used as feedback to accurately time the droplet injections. The presented system is contrasted to attempts without feedback, and is shown to be 100% reliable over long durations. Additionally, content detection and discretionary injections are explored and successfully executed.

Keywords Droplet microfluidics · Droplet detection · Impedance · Feedback control

✉ Tza-Huei Wang
  thwang@jhu.edu

[1] Department of Biomedical Engineering, Johns Hopkins University, 3400 N. Charles Street, Clark Hall 118B, Baltimore, MD 21218, USA

[2] Department of Mechanical Engineering, Johns Hopkins University, 3400 N. Charles Street, Shaffer Hall 200A, Baltimore, MD 21218, USA

1 Introduction

Droplet based microfluidics, since its inception almost two decades ago, has been highly valued in biological applications for its ability to increase throughput while simultaneously reducing reagent consumption and decreasing reaction times (Burns et al. 1998; Teh et al. 2008; Thorsen et al. 2001). Even when compared to conventional minute fluid volume handling methods such as microtiter plates, droplet microfluidics has the potential to drastically lower processing cost and improve outcomes as it avoids sample loss from pipetting and non-specific adsorption (Dunn and Feygin 2000; Warrick et al. 2007; Yin et al. 2008). The lack of a physical barrier enclosing each reaction volume, within droplets, affords its critical advantage even over other microfluidic assay systems of avoiding loss of vital reaction components to surface adsorption. Additionally, each individual droplet in the device acts as a separate reaction isolate which lends itself naturally towards parallelization of assays or digital processing of bulk fluids (Vyawahare et al. 2010). Benefitting from this, some of the recent applications of droplet microfluidics include single molecule analysis (Guan et al. 2015; Rane et al. 2015a; Weinmeister et al. 2015), single-cell analysis and sorting (Mazutis et al. 2013; Rane et al. 2012), disease detection (Juul et al. 2012; Zec et al. 2014), and enzyme kinematic studies (Hess et al. 2015). These fields have a need for platforms that are low-cost and high-throughput with streamlined controlled

sample sequences, short analysis times, and accurate tools for analyzing various biological moieties. Droplet microfluidics encapsulates most of these desired characteristics, but they also inherit certain challenges, such as efficient droplet manipulation and tracking post-generation.

One specific challenge of droplet manipulation is addition of reagent further downstream from droplet creation. Reagent mixing is a fundamental part of many assays, single cell analyses, or diagnostics. Various groups have created passive injection systems that allows for high frequency droplet merging, but lack programmability to create combinatorial screening (Niu et al. 2008; Tan et al. 2004). To overcome these limitations, several active merging techniques have been developed such as electrocoalescence (Abate et al. 2010; Zagnoni and Cooper 2009), surface acoustic wave merging (Sesen et al. 2014), pneumatic actuators (Yoon et al. 2014), and magnetic fields (Varma et al. 2016). Some of these techniques have been used to create on-demand combinatorial assays have been demonstrated using on-chip microfluidic valves (Hsieh et al. 2015; Rane et al. 2015b; Zec et al. 2012), off-chip mechanical valves (Tangen et al. 2015), and electrocoalescence picoinjectors (Abate et al. 2010). However, without an efficient feedback network the droplets must be merged during or soon after droplet generation, and these combinatorial assays are limited to single step complexity. One group has demonstrated potential for downstream combinatorial droplet merging with feedback control through the use of a fluorescent microscope and picoinjectors (Abate et al. 2010). However, the need for a complex optical detection system mounted on an inverted microscope, in addition to the droplet requiring fluorescent molecules to enable detection, reduces the applicability of the system. Furthermore, the efficacy and limitations of the system have not been evaluated.

Electrochemical methods of measurement are an attractive alternative as they are easy to fabricate using the same technology as the microfluidic device; they can be more easily minimized; and they have the added bonus of being able to control droplets through techniques like dielectrophoresis (Valero et al. 2010) and electrocoalescence (Zagnoni and Cooper 2009). Impedance-based detection platforms rely on the change in capacitance of coplanar electrodes as a droplet travels across them (Bhattacharjee and Najjaran 2012), and has been employed to perform content detection like real-time DNA amplification (Fang et al. 2013).

In this regard, we present a highly sensitive system capable of tracking droplets in a multiphasic environment, using impedance, for the purpose of successful on-demand addition of reagents to isolated sub-microliter droplets with great precision.

2 Methods and materials

2.1 Microdevice design and overview

The microfluidic device used in this study and its operations are detailed in Fig. 1, with an annotated photograph of the prototype device and expanded illustrations of each functional region. The droplet generation region of the microdevice (Fig. 1a), is capable of generating droplets of any combination from three fluid inlets, each moderated by microfluidic valves. On either side of these fluid inputs are two pressure relief valves, marked P1 and P2 in Fig. 1a, that open during droplet creation to alleviate any pressure drop across the fluid inlets. These inlets generate droplets by opening the valve to let sample flow into the main channel, and then shutting the valve to separate the droplet from the bulk fluid. The applied pressure at the inlets and duration of valve opening dictate the size of the droplet, thus allowing for droplets to be generated on-demand, with their size precisely tuned (Zeng et al. 2009). One of the reagent inlets (Fig. 1b) has an attached rinsing channel that allows for multiple plugs to be loaded into the channels without pausing device operation. The droplets thus created enter the first of two incubation regions, as depicted in Fig. 1c. This travel region in the device simulates a long processing step, such as mixing or incubation facilitating a reaction that the droplet could undergo in an assay. This region also doubles its functionality as a fluid buffer to dampen the effects of any sudden pressure variation during droplet creation or injection. Figure 1d is an illustration of the detection and injection region, where traveling droplets are identified and merged with additional reagents. The presented microdevice design includes three inlets in the injection region, for up to three different reagent additions, and it can be easily expanded to meet analysis needs. Just upstream of these reagent inlets is a pair of coplanar electrodes that transversely cross the fluid channel. The impedance signal (its phase component shown in Fig. 1d) measured across these electrodes is analyzed to detect the presence of a droplet. This information is used to time the actuation of the microfluidic valves so that successful addition of reagent occurs.

2.2 Device fabrication

The microdevice in this study consists of three functional layers: the substrate with electrodes, the fluid layer, and the valve control layer. The detailed fabrication steps involved in assembling this device are illustrated in Fig. 2, and further detailed below.

Electrode deposition The gold electrodes are patterned onto a 75x50x1mm glass slide (Cat. No.2947-75X50, Corning) using electron-beam deposition and liftoff techniques. In brief, the glass slides are cleaned in acetone, followed by
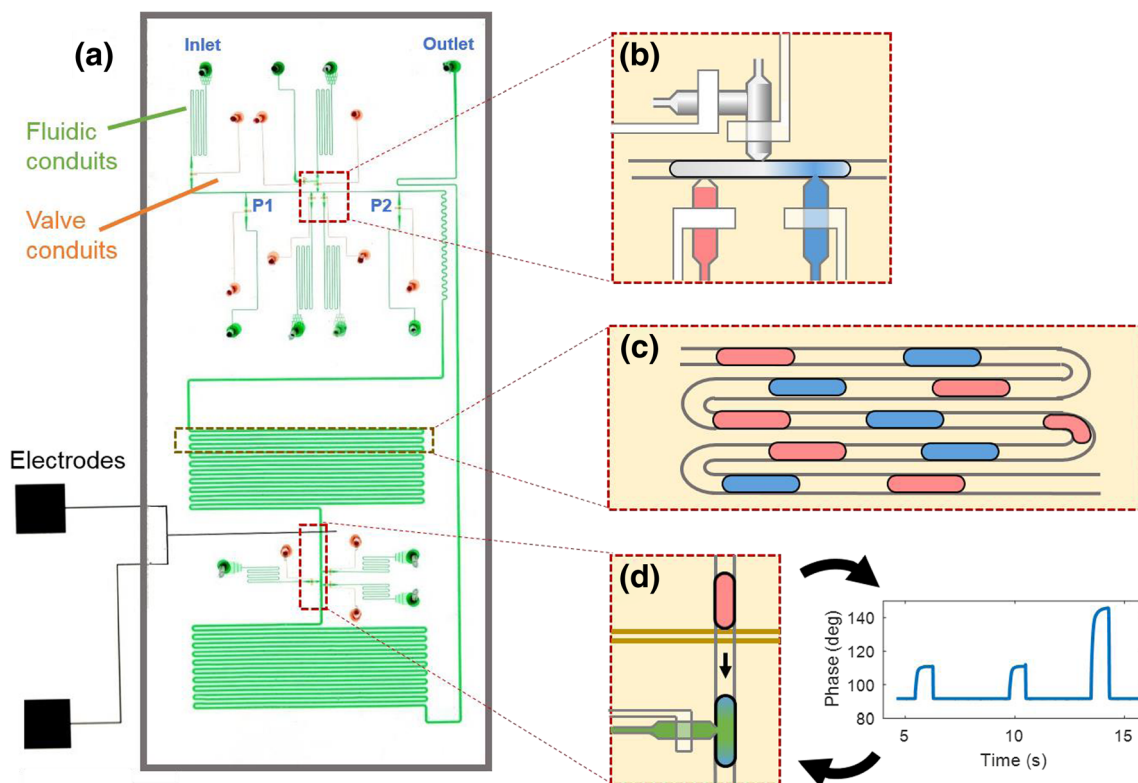
Fig. 1 Overview of the microfluidic device layout. **a** A digital image of the device prototype with its three different layers highlighted – the fluid channels dyed green, the valve control channels dyed orange, and the electrodes solid black. The three functional regions of the chip, which are outlined in inserts, are detailed as schematics (**b**) (**c**) and (**d**). **b** The droplet generation region, with three potential inlets to create sample droplets. One of the inlets on the top has an attached rinsing channel that allows for switching samples without cross-contamination; (**c**) the incubation region, to simulate a long processing step that could occur; and (**d**) the detection and injection region, where droplet sensing and mixing occurs. The electrode is placed after the first incubation region, upstream of a reagent inlet. When droplets of a particular composition (*marked blue*) passes by, the valve controlling the inlet is actuated and the reagent (*marked green*) is directly injected into the passing droplets. A sample plot of the corresponding phase change in the impedance signal is shown. This signal is used to detect and actuate the reagent inlets to time the injections

isopropanol rinse, and subsequent exposure to oxygen plasma for 3 min at 100 watts. Positive photoresist (Microposit® S1813, Microchem Inc.) is spun onto the clean glass slides at 2000 rpm for 30 s, soft baked at 115 °C for 90 s, and exposed to UV light at 150 mJ/cm^2 for 30 s during contact photolithography. The glass slide is then immersed in a developer bath (Microposit® MF® CD-26, Microchem Inc.) to reveal the pattern for the electrodes on the glass. A 50 nm layer of chrome is deposited on top of the photoresist in an e-beam evaporator, followed by a 500 nm layer of gold. The underlying photoresist is then lifted off using acetone, leaving the finished substrate layer with the patterned gold electrodes.

Template microfabrication The templates for the fluid layer and the valve control layer are fabricated using SU-8 and SPR photoresists. The fluid layer involves two steps of photolithography to make the rectangular fluid channels and the rounded collapsible valve channels. This process was detailed previously by Quake Labs (Unger et al. 2000), but briefly, positive photoresist (Microposit® SPR-220, Microchem Inc.) is first spun on to a thickness of 20 μm, patterned into valve

channels 100 μm wide, and hard baked. Then a negative photoresist (Microposit® SU-8 2030, Microchem Inc.) is spun on to a thickness of 20 μm, patterned for the remaining fluidic channels, and hard baked. After the development process, the positive photoresist leaves behind rounded channel cross-sections that facilitate collapse, whereas the negative photoresists have rectangular cross-sectional geometry. The width of the channels range from 50 μm in the droplet creation region to 200 μm in the incubation region. The narrower channel in the droplet creation region serves to elongate the droplets to facilitate combinatorial droplet mixing. For the valve control layer template, a single layer of negative photoresist (Microposit® SU-8 2030, Microchem Inc.) is spun on to a silicon wafer with a thickness of 20 μm and patterned into the control channels.

Soft lithography Corresponding molds of the fluidic and valve layers patterns are made in PDMS. For the valve control layer, a 6:1 ratio of prepolymer to curing agent is spun onto the template at 100 rpm for 2 min followed by a 5-min bake at 80 °C. Alternatively for the fluid layer, PDMS at 15:1 ratio is

Fig. 2 Schematic detailing the fabrication steps in assembling the microdevice. The three columns (*from left to right*) feature the patterned deposition of electrodes on a glass substrate, and the two PDMS layers comprising the fluidic and valve channel layouts. Not shown are the photolithography steps for the creation of the master molds for the latter two layers. The final two schematics depict the three layers aligned and bonded irreversibly using oxygen plasma, with tubes providing access to the microfluidic network of channels in the fluidic and valve control layers. The entire microdevice is then treated with a hydrophobic coating, to ensure smooth movement of the droplets traversing the electrode surface
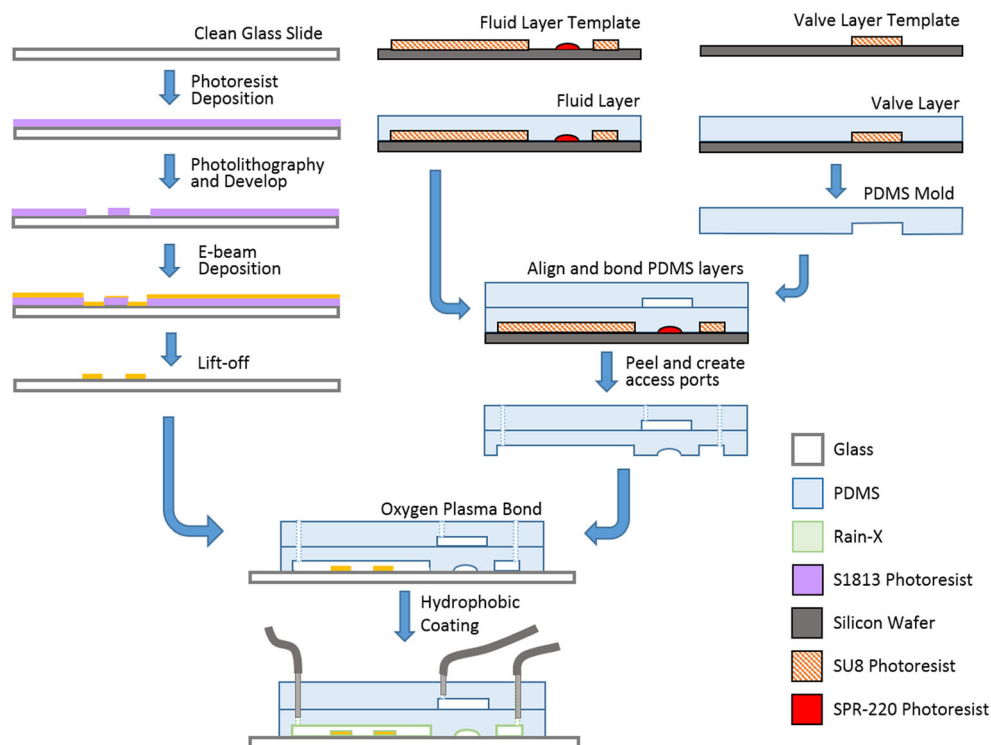
spun at 1300 rpm for 1 min followed by a 4-min bake at 80 °C, yielding a thin PDMS sheet on top of the fluid layer mold that collapses when the valve control layer is pressurized.

Chip assembly Initially the PDMS valve control layer is peeled off of the template and aligned on top of the fluid layer (Fig. 2). The two PDMS layers are allowed to bond permanently by baking for 7 h at 80 °C. An additional layer of 10:1 PDMS is poured over the bonded layers and cured to increase the device thickness to better support the fluidic connectors. The multi-layered PDMS assembly is then peeled off the fluid template and access ports are created for the valves and channels. It is then aligned and oxygen-plasma-bonded (60 s at 30 W) to the glass slide patterned with the gold electrodes. The complete microdevice is then baked for a minimum of 5 h at 80 °C to ensure a robust bonding of the multiple layers.

Pretreatment and surface modification Prior to each test trial, the PDMS and glass surfaces of the fluid channels are made hydrophobic through application of a commercial hydrophobic coating agent (Rain-X® Original, ITW Global Brands). Initially, the microdevice is exposed to oxygen plasma for 45 s at 30 W. Then, the fluid channels are perfused with the hydrophobic coating and allowed to set for 5 min, before being flushed with air and dried at room temperature.

2.3 Components of the test system

Valve control system The microfluidic valves were adapted from a previously described method from Quake Laboratories[8]. These valves are actuated pneumatically by an array of solenoid valves that are controlled by MATLAB software, which also receives impedance measurements. The valve control layer is connected to the solenoid valves by a length of Tygon® tubing (Cole-Palmer) filled with water that allows the PDMS valves to actuate faster.

Impedance measurement circuit The electrodes on the device are designed to behave as a coplanar capacitor, dependent on the dielectric properties of the surrounding material. A four terminal measurement system is implemented to measure the impedance between these electrodes, wherein the current through the capacitor and voltage drop across them are measured independently to increase measurement accuracy. The entire circuit for measurement is illustrated in Fig. 3. Probes are attached to the gold electrodes on the microdevice using an electrically conductive epoxy (8331S, MG Chemicals). A high impedance differential amplifier within the spectroscope is used to measure the voltage across the electrodes without drawing current, while a trans-impedance amplifier (HF2TA, Zurich Instruments) converts the current passing through the electrodes to a voltage signal for sampling. A set of commercial dual-phase demodulators (HF2IS, Zurich Instruments) read the voltage signals and store the real and imaginary
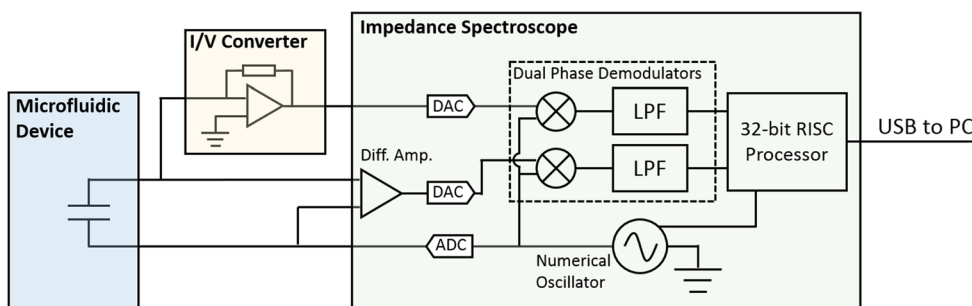
Fig. 3 Circuit architecture for the impedance measurement circuit. The impedance spectroscope (HF2IS, Zurich Instruments) generates a signal internally from a numerical oscillator which is transformed into an analog signal by a digital-to-analog converter (DAC). In a four terminal configuration, the voltage drop across the electrodes in the microfluidic device is measured through a high impedance differential amplifier internal to the impedance spectroscope. This signal is then converted with an analog-to-digital converter (ADC) before being passed into a dual phase demodulator that outputs values proportional to the real and imaginary components of the signal. This value, stored in a register of a 32-bit processor, can be accessed by a computer. Current through the electrodes is converted to a voltage signal by an I/V converter (a trans-impedance amplifier). It is then similarly passed through an ADC before being split into signal components by a dual phase modular. Internally, the dual phase modulators consist of signal multipliers followed by low pass filters to get voltage signals proportional to the real and imaginary components of the sine waves

components into memory to be accessed at any time by a connected computer via a USB interface.

Software for droplet identification The software used to automate the microfluidic system was written in MATLAB for the purpose of completing the feedback-control loop. It periodically samples the impedance of the electrodes and controls the microfluidic valves in response. The process of analyzing the signal for injection is illustrated in Fig. 4. There are four stages of each successful injection as depicted in Fig. 4a-d: a droplet detection event; a delay period; an injection period; and a refractory period. Firstly the detection event, when a droplet first reaches the electrodes it appears as a fluctuation in recorded impedance values, both in magnitude and phase.

Threshold detection is employed to detect this change and therefore the droplet. Secondly, the delay period is the time between the detection event and the droplet injection which allows the droplet to travel from the electrodes to the corresponding reagent valve. Thirdly, the injection timer is the duration of reagent valve opening for fluid injection. And lastly, the refractory period is the time where no measurement is made on the electrode to accommodate the possibility of droplets expanding backwards over the electrodes during a large injection. This prevents a false droplet detection event, but for most situations the timer is set to zero seconds.

Imaging and analysis During the experimental trial, the microdevice was mounted on an inverted microscope (IX71,
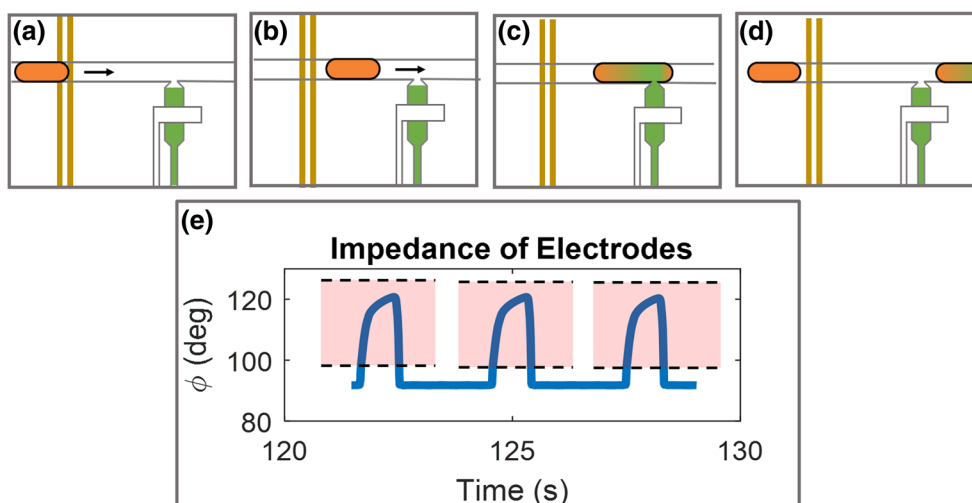
Fig. 4 Illustration of stages in droplet detection and injection. **a** The detection event where the droplet initially reaches the electrodes. This correlates to a rise in the impedance phase as depicted in 4(**e**). **b** The droplet travel during the 'delay time' period. **c** The 'open time' period where the droplets are merged with reagent. **d** The 'refractory time' period during which the impedance measurements are ignored in order to prevent false positive detection. **e** A graph illustrating the change in impedance phase signal over time, as a droplet travels across the electrodes. The pink regions represent the thresholds used to identify the presence of the droplet and the gaps represent the refractory period where the signal readout is ignored

Olympus) for observation. A camera (70D, Canon™) was affixed to the microscope to capture video of its operation. Video tracking software (Tracker, Douglas Brown) was used to track the position of the droplets.

2.4 Experimental conditions

The continuous phase in the droplet trials constitutes a silicone oil mix (1:4 mixture of PFO in FC-40), and the samples for the droplets were created from deionized (DI) water or phosphate buffered saline (PBS). The samples were occasionally mixed with food dye to assist visual tracking of droplets for analysis and presentation.

The preliminary set of experiments was aimed at characterizing the system and determining an optimal measuring frequency. With impedance being a frequency-dependent property, and inability to measure all frequencies simultaneously, frequency choice is necessary to conduct real-time measurements. Frequency sweeps were performed on stationary droplets of DI water using commercial software included with the impedance spectroscope (ziContro, Zurich Instruments) from 10 kHz to 3 MHz. The sweep was then repeated on the surrounding silicone oil mixture. The frequency where the two fluids were most distinct was chosen as the operating frequency of the system. After the sweep on stationary droplets, a few select frequencies were chosen to measure the impedance of traveling droplets to assure that measurements were consistent with operating conditions. For the traveling impedance measurements, droplets were generated at 0.5 Hz frequency, and at least 5 droplets' signals were measured at each selected frequency. The peak value of each signal was recorded, and the average peak signal of all the droplets was plotted over the stationary sweeps for comparison.

The following set of trials were designed to demonstrate the uncertainty in identifying droplet position that exists in an open-loop control environment. The goal was to qualitatively determine the benefits of feedback-control systems compared to open-loop systems. For instance, it has been shown in literature that the presence of droplets within a microfluidic device affects the downstream resistance to fluid flow in pressure-driven devices (Baroud et al. 2010). Consequently, in our pressure-driven device, the speed of the droplets, and therefore their predicted positions, would be affected by the amount of droplets populating the device at any given instance. In order to understand this effect, droplets of DI water were generated at 0.2 Hz, and speed of the droplets within the main fluid channel was measured after each droplet creation to determine the relationship between net droplet count and the speed of droplets traversing the system. Additionally, the transient behavior of droplets in the main fluid channel during a droplet creation was recorded for analysis.

A comparison of the performance between the open-loop control and feedback control systems was made at steady state operating conditions. At steady state, the frequency of droplets exiting the device is equal to the frequency at which they are created, thus eliminating the uncertainty in droplet position stemming from the varying number of droplets in the device. Furthermore, injected droplets were allowed to fill the second incubation zone and begin leaving the device to avoid additional pressure variation induced by a change in droplet size post-injection. Lastly, the frequency of injection was finely tuned to allow for the maximum possible consecutive successful injections (at least ten consecutive droplets). Once the above trial conditions were achieved, the following 100 droplets were observed and the number of successful injections recorded. The trial was repeated for the system with feedback control in order to compare the rates of successful injections.

The final set of trials focused on investigating the capabilities of the impedance-based feedback system for droplet content detection and discretionary injection. For this, two samples comprising of DI water mixed with green food dye and 10× PBS mixed with red food dye (1:10 ratio), were used to create droplets in the droplet generation region of the microdevice. Droplets of these samples were generated at 0.2 Hz in a predetermined patterned repeats, and the impedance detection was utilized to selectively inject PBS droplets in various dictated combinatorial patterns. Upon completion of the test, the flow was stopped to capture a panoramic photograph of the device, for analysis.

3 Results and discussion

3.1 System characterization

Frequency sweep data of the stationary droplet was compared to the peak values observed in traveling droplets (Supplementary Fig. 1a). The optimal measurement frequency to distinguish the silicone oil mixture from DI water was determined to be between 10 kHz and 50 kHz. Additionally, it was observed that the peak measurements of the traveling droplets followed the stationary sweeping data narrowly. It was therefore inferred that a quick stationary sweep to determine the appropriate measurements of frequency to distinguish the continuous phase from the dispersed phase would suffice, for a new combination of immiscible fluids. In Supplementary Fig. 1b, shows a sample plot of the impedance signal at 200 kHz of droplets travelling across the electrodes. Since any movement of the microscope stage or disturbances of the coaxial cables during experimentation translated to a variation in the magnitude of the impedance measurement, while the phase measurements remained unaffected, it was decided to use the latter (phase change of the impedance signal) for threshold detection.

3.2 Droplet velocity uncertainty

The predictability of a droplet's position in a device with high accuracy is very critical to have a reliable open-loop control downstream injection. In order to evaluate the efficacy of predicting droplet movement, the velocity of droplets through the device was measured as a function of the number of droplets in the fluidic channel. The resulting relationship between droplet velocity and droplet count is shown in Supplementary Fig. 2. Supplementary Fig. 2a highlights the near linear relationship of droplet speed and the number of droplets present in the device over a large range. Therefore, the knowledge of the exact number of droplets in the device at all times is critical in accurately ascertaining the droplet travel time over large distances. Additionally, it was observed that this speed change is not instantaneous, and has some transience that must be accounted for as well. When the relief valves open during droplet generation, there is a temporary transience in the speed of the droplets throughout the device, as shown in Supplementary Fig. b. Although this change in speed is more dramatic in droplets closest to the relief valves, the effect is still noticeable in droplets farther away. Together, this data reveals the difficulties in predicting droplet position in microdevices with long droplet travel.

3.3 Feedback vs non-feedback in an optimized setting

Although many uncertainties in droplet position is dependent on steady state conditions, it was suspected that even in steady state conditions, open-loop control systems would have difficulty with successful injections due to numerous unknown compounding factors. In order to analyze this effect, we tested a microdevice operating in steady state and attempted to inject traveling droplets with an injection activated at regular time intervals. The results of this attempt compared to the feedback system are captured in Fig. 5.

Figure 5a displays images of droplet injections at the start of the 100-drop attempt for both open-loop control and feedback control trials. After multiple attempts at open-loop injection success, the best result that could be obtained was 15 successful consecutive injections, before the injection began to miss. This is contrasted with the same attempt with an active feedback system. After over 100 droplets, the feedback control system never missed an injection, as communicated in Fig. 5b.

3.4 Content detection and discriminatory injection

In order to further investigate the capabilities of this system for droplet content detection, control droplets (DI water with green dye) and PBS droplets (with red dye) were generated in a pattern of two PBS droplets in sequence followed by a single control droplet. The measurement frequency was 200 kHz, and DI water mixed with blue food dye was used as the reagent of choice for injection. A resulting sample of the impedance signal demonstrates the difference in impedance signal as is shown in Fig. 6a.

Threshold detection was employed to dictate the injection of only the PBS droplets in the sequence with blue dye. After a sequence of over 100 droplets, injection attempts were

Fig. 5 Evaluating efficacy of the feedback system. **a** Series of images demonstrating the reliability of the feedback system in contrast to the performance of the non-feedback system. The images are captured beginning with the attempted injections. The best result obtained without feedback was 15 successful injections before a 'miss' occurred. **b** The feedback and non-feedback systems were allowed to run for a series of 100 consecutive droplets, and assessed for their outcomes. The pie charts represent the fraction of successful injections as compared to all attempted injections
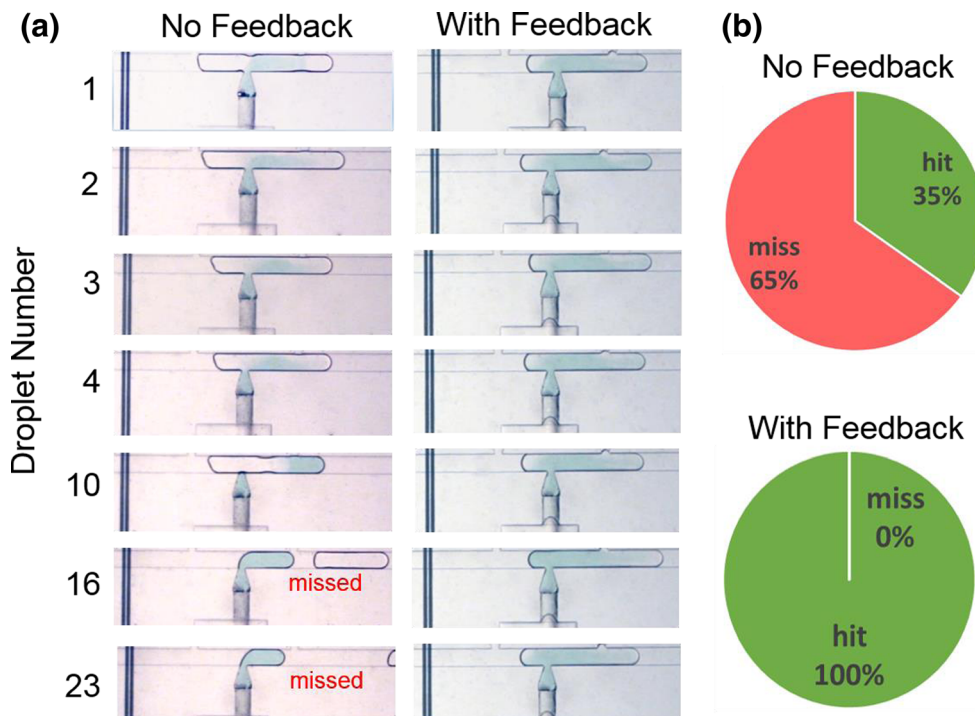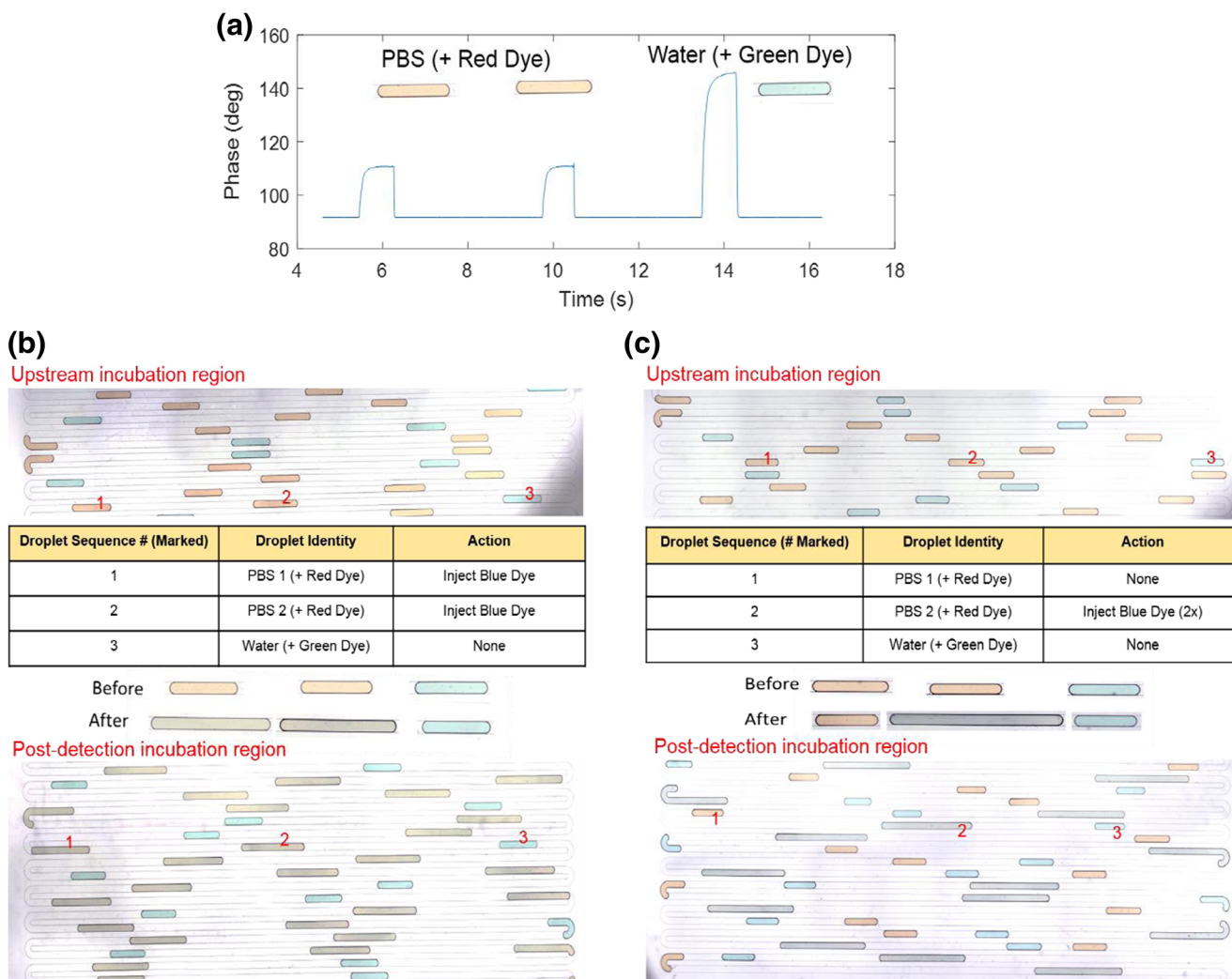
Fig. 6 Demonstration of versatility of the feedback system. This figure illustrates the versatility of the feedback system in injecting on-demand content of the droplets as well as sequencing. In this trial, samples of green and red food dyes were mixed at 1:10 ratio, with water and 10× PBS respectively. **a** A snapshot of the impedance signal variation as droplets, in a pre-determined sequence of two PBS droplets followed by one water droplet, travel past the electrodes. **b** A panoramic image of the two incubation regions of the device when every PBS droplet was dictated to be mixed with blue dye. Successful addition of blue dye to each PBS droplet, post-detection at the electrodes, can be observed in the droplets populating the downstream incubation region, as changes in droplet color and droplet size (increase). (c) A panoramic image of the device, under a similar trial with instructions to inject only the 2nd PBS droplet, in each repeat sequence, with blue dye after detected by the electrodes. This demonstrates the multiplexing capabilities of this system, in that the first PBS droplet that was 'ignored' of an injection could represent a control droplet while the blue (reagent)-injected droplet could be the test sample. Alternatively, the 1st PBS droplet could be injected with a separate reagent to carry out dual assays

analyzed to determine that 100% specificity and injection accuracy was achieved. There were no green droplets that received the blue injection, and there were no red droplets that missed an injection (Fig. 6). The flow of oil was stopped and a panorama photograph of the device along with example before and after sequences is shown in Fig. 6b. To additionally demonstrate the combinatorial capabilities of this technology, the microdevice was flushed with oil and the software was rewritten to only inject the first PBS droplet, in each sequence repeat, with blue dye. Once again, the system had 100% specificity and 100% accuracy as highlighted in Fig. 6c. In summary of this trial, there were no instances of the first PBS droplet not receiving an injection, and no instances of the second PBS droplet receiving an injection.

4 Conclusions

In this paper, a novel feedback control system for droplet-based microfluidic devices with microfluidic valves is presented. The system utilizes real-time impedance measurements of on-chip electrodes to control microfluidic valves for accurate downstream injections. The system was calibrated to track DI water droplets and PBS

droplets suspended in silicone oil. Results indicated that the droplets were accurately located and identified as they traveled through the microfluidic device. Furthermore, the uncertainty of droplet dynamics during long processing distances was demonstrated to justify the need for feedback control in downstream injection sites. Among the most important of these uncertainties was the downstream resistance to flow, as it was dependent on the number of droplets present within the device. But, even in the absence of this factor the efficiency of predicting droplet position for successful injections was very low with an open-loop control system. The presented feedback system is effective in overcoming these challenges successfully, and reliably mixing droplets with desired reagents. With this system in place, long duration experiments could potentially be executed without human interference to consistently and reliable mix reagents downstream. In addition, it was further presented that the functionality of this control system extends beyond basic positional detection to provide information about the droplet content as well. It was demonstrated that droplets could be discretionally mixed in a combinatorial manner dependent upon their electrical properties.

Potential future applications of this technology lie in application to biological assays on-chip which require multiple additive steps or extremely long run times. It could now be possible to run overnight assays with confidence that would otherwise require constant monitoring. Additionally, the sensitivity of the impedance measurements could be further improved to detect more detailed content within the microfluidic droplets. This would allow for detection of post assay products to determine earlier processing success before using reagents to perform mixing, resulting in even greater material savings in high-throughput experimentation.

References

A.R. Abate, T. Hung, P. Mary, J.J. Agresti, D.A. Weitz, Proc. Natl. Acad. Sci. U. S. A. **107**, 19163 (2010)

C.N. Baroud, F. Gallaire, R. Dangla, Lab Chip **10**, 2032 (2010)

B. Bhattacharjee, H. Najjaran, Lab Chip **12**, 4416 (2012)

M.A. Burns, B.N. Johnson, S.N. Brahmasandra, K. Handique, J.R. Webster, M. Krishnan, T.S. Sammarco, P.M. Man, D. Jones, D. Heldsinger, C.H. Mastrangelo, D.T. Burke, Science **282**, 484 (1998)

D.A. Dunn, I. Feygin, Drug Discov. Today **5**, S84 (2000)

X. Fang, Q. Jin, F. Jing, H. Zhang, F. Zhang, H. Mao, B. Xu, J. Zhao, Biosens. Bioelectron. **44**, 241 (2013)

W. Guan, L. Chen, T.D. Rane, T.H. Wang, Sci. Rep. **5**, 13795 (2015)

D. Hess, A. Rane, A.J. Demello, S. Stavrakis, Anal. Chem. **87**, 4965 (2015)

K. Hsieh, H. Zec, P. Ma, T. Rane, T.H. Wang, Micromachines **6**, 1490 (2015)

S. Juul, C.J.F. Nielsen, R. Labouriau, A. Roy, C. Tesauro, P.W. Jensen, C. Harmsen, E.L. Kristoffersen, Y. Chiu, R. Frøhlich, P. Fiorani, J. Cox-Singh, D. Tordrup, J. Koch, A.L. Bienvenu, A. Desideri, S. Picot, E. Petersen, K.W. Leong, Y.P. Ho, M. Stougaard, and B.R. Knudsen, ACS Nano. **6**, 10676 (2012)

L. Mazutis, J. Gilbert, W.L. Ung, D.A. Weitz, A.D. Griffiths, J.A. Heyman, Nat. Protoc. **8**, 870 (2013)

X. Niu, S. Gulati, J.B. Edel, A.J. DeMello, Lab Chip **8**, 1837 (2008)

T.D. Rane, H.C. Zec, C. Puleo, A.P. Lee, and T.H. Wang, Lab Chip **12**, 3341 (2012)

T.D. Rane, L. Chen, H.C. Zec, T.H. Wang, Lab Chip **15**, 776 (2015a)

T.D. Rane, H.C. Zec, T.H. Wang, Anal. Chem. **87**, 1950 (2015b)

M. Sesen, T. Alan, A. Neild, Lab Chip **14**, 3325 (2014)

Y.C. Tan, J.S. Fisher, A.I. Lee, V. Cristini, A.P. Lee, Lab Chip **4**, 292 (2004)

U. Tangen, A. Sharma, P. Wagler, J.S. McCaskill, Biomicrofluidics **9**, 1 (2015)

S.Y. Teh, R. Lin, L.H. Hung, A.P. Lee, Lab Chip **8**, 198 (2008)

T. Thorsen, R.W. Roberts, F.H. Arnold, S.R. Quake, Phys. Rev. Lett. **86**, 4163 (2001)

M.A. Unger, H.P. Chou, T. Thorsen, A. Scherer, S.R. Quake, Science **288**, 113 (2000)

A. Valero, T. Braschler, N. Demierre, P. Renaud, Biomicrofluidics **4**, 1 (2010)

V.B. Varma, A. Ray, Z.M. Wang, Z.P. Wang, R.V. Ramanujan, Sci. Rep. **6**, 37671 (2016)

S. Vyawahare, A.D. Griffiths, C.A. Merten, Chem. Biol. **17**, 1052 (2010)

J. Warrick, I. Meyvantsson, J. Ju, D.J. Beebe, Lab Chip **7**, 316 (2007)

R. Weinmeister, E. Freeman, I.C. Eperon, A.M. Stuart, A.J. Hudson, ACS Nano **9**, 9718 (2015)

H. Yin, N. Pattrick, X. Zhang, N. Klauke, H.C. Cordingley, S.J. Haswell, J.M. Cooper, Anal. Chem. **80**, 179 (2008)

D.H. Yoon, A. Jamshaid, J. Ito, A. Nakahara, D. Tanaka, T. Akitsu, T. Sekiguchi, S. Shoji, Lab Chip **14**, 3050 (2014)

M. Zagnoni, J.M. Cooper, Lab Chip **9**, 2652 (2009)

H. Zec, T.D. Rane, T.H. Wang, Lab Chip **12**, 3055 (2012)

H. Zec, D.J. Shin, T.H. Wang, Expert. Rev. Mol. Diagn. **14**, 787 (2014)

S. Zeng, B. Li, X. Su, J. Qin, B. Lin, Lab Chip **9**, 1340 (2009)